

# Neutron Production by 0.8 and 1.5 GeV Protons on Fe and Pb Targets at the Most-Forward Region

Daiki SATOH<sup>\*</sup>, Nobuhiro SHIGYO<sup>1</sup>, Kenji ISHIBASHI<sup>1</sup>, Yasushi TAKAYAMA<sup>1</sup>,  
Shunsuke ISHIMOTO<sup>1</sup>, Yosuke IWAMOTO<sup>1</sup>, Hideki TENZOU<sup>1</sup>, Tatsushi NAKAMOTO<sup>2</sup>,  
Masaharu NUMAJIRI<sup>2</sup> and Shin-ichiro MEIGO<sup>2</sup>

<sup>1</sup>Department of Applied Quantum Physics and Nuclear Engineering, Kyushu University,  
6-10-1 Hakozaki, Higashi-ku, Fukuoka 812-8581, Japan  
email: satoh@meteor.nucl.kyushu-u.ac.jp

<sup>2</sup>High Energy Accelerator Research Organization, 1-1 Oho, Tsukuba 305-0801, Japan

<sup>3</sup>Japan Atomic Energy Research Institute, Tokai-mura, Ibaraki 319-1195, Japan

Neutron-production double-differential cross-sections for 0.8 and 1.5 GeV protons incident on Fe and Pb targets were measured at the most-forward region. Neutrons were measured by the time-of-flight (TOF) method. An NE213 liquid organic scintillator was set at 0-degree as neutron detector. Neutron detection efficiencies are calculated by a Monte Carlo simulation code SCINFUL-QMD. Experimental data were compared with other experimental data and the results of calculation codes based on Intranuclear-Cascade-Evaporation (INC/E) and Quantum Molecular Dynamics (QMD) models. Disagreement with the codes is discussed.

## 1. Introduction

Studies on spallation reaction have recently been made for various applications, such as spallation neutron source and Accelerator-Driven-System (ADS) for transmutation of nuclear waste or energy-production. For example, projects for intense neutron sources based on the proton-incident spallation reaction have been proposed in Japan (Japan Proton Accelerator Research Complex; J-PARC[1]), USA (National Spallation Neutron Source; SNS[2]) and Europe (European Spallation Source; ESS[3]).

For the design of these facilities, evaluated nuclear data in the energy region up to a few GeV are required. Compilation of the high energy nuclear data files is carrying out in the world, for instance, JENDL High Energy File[4] (JENDL-HE, Japan), LANL High Energy File[5] (LA-150, USA), Medium Energy Nuclear Data Library[6] (MENDL-2, Russia). Nuclear data evaluation is generally performed on the basis of experimental data and theoretical model calculations. However, the experimental data are sparse and unsatisfied. Theoretical model calculations play, therefore, an important role. Intranuclear-Cascade-Evaporation (INC/E) model[7] and Quantum Molecular Dynamics (QMD) model[8] have often been utilized in the energy region above a few hundred MeV. Although improvement of the calculation codes have been performed, some discrepancies still remain between experimental data and model predictions. In general, calculation codes tend to fail to reproduce the neutron-production double-differential cross-sections in the most-forward region. Theoretical models employed in these codes cannot treat correctly a collective-effect such as the analog of a giant resonance accompanied with the isospin flip. Experimental data are required to improve the model precision in this region.

Measurement of neutron-production double-differential cross-sections in the most-forward direction has been carried out by the time-of-flight (TOF) method at the  $\pi 2$  beam line of 12-GeV proton synchrotron (12-

GeV PS) in the High Energy Accelerator Research Organization (KEK). At KEK, we have already measured neutron-production double-differential cross-sections by the TOF method, except for 0-degree measurement. The detail of those experiments was written in our previous reports[9,10].

The recoil proton method combined with a magnetic spectrometer has been often utilized for 0° neutron spectrum measurement[11,12], because TOF technique has a poor energy resolution for high energy neutrons. The TOF method, however, owns a higher detection efficiency and simpler data analysis than the recoil proton method. Since the beam intensity at the  $\pi 2$  beam line is very weak, we adopted TOF technique as the neutron detection method. For obtaining the better experimental data, the improvement of energy resolution in the measurement is essential. A high-resolution TOF method was devised to meet this demand: three rapid-rise-time photomultipliers were connected with a neutron detector.

In this work, we report the results of 0-degree measurement by the high-resolution TOF method. Cross sections were obtained on targets of Fe and Pb at incident proton energies of 0.8 and 1.5 GeV. We aimed at measuring the emitted neutrons above a few hundred MeV because of the experimental constraint. Comparisons are made between the experimental data and the results of calculation codes, NMTC/JAM[13] based on INC/E model and JQMD[14] on QMD model.

## 2. Experimental method

The experiment was carried out at the  $\pi 2$  beam line of 12-GeV PS at KEK. Schematic view of the experimental arrangement is shown in Fig. 1. NE102A plastic scintillators were set in front of the target to define the incident proton beam area. The coincidence of signals from these scintillators was counted to determine the number of incident particles. The incident beam was deflected at the downstream of the target with electric bending magnet in order to prevent it from being incident on the 0° detector. Since the vertical gap between the magnetic poles was narrow (30 cm), secondary scattering of emitted particles takes place on the magnet pole piece. It was difficult to set the shielding between the electric bending magnet and the neutron detector, without giving influence to neutrons of interest. Therefore, the measurement was made without the shielding.

The Fe and Pb targets was bombarded by the proton beam. Targets were cylindrical disk with a diameter of 50 mm. The thickness of Fe and Pb targets was 30 and 20 mm, respectively. NE213 liquid organic scintillator was employed as neutron detector. The shape was cylinder 12.7 cm in diameter and 12.7 cm thick. The neutron detector was placed at 0°. For improvement of the energy resolution, photomultipliers of fast rise time (Hamamatsu H2431, rise time 0.7 ns) were adopted. Three H2431s 5.1 cm in diameter were connected with the NE213 scintillator. The neutron arrival time was obtained by time-average of three photomultipliers to give the best time resolution. Flight path length was 3.5 and 5.0 m for 0.8 and 1.5 GeV proton incidence, respectively. In front of the neutron detector, NE102A scintillator was mounted as a veto detector to reject the charged particle events. Background measurements were performed without target to subtract the neutrons produced from the beam scintillators.

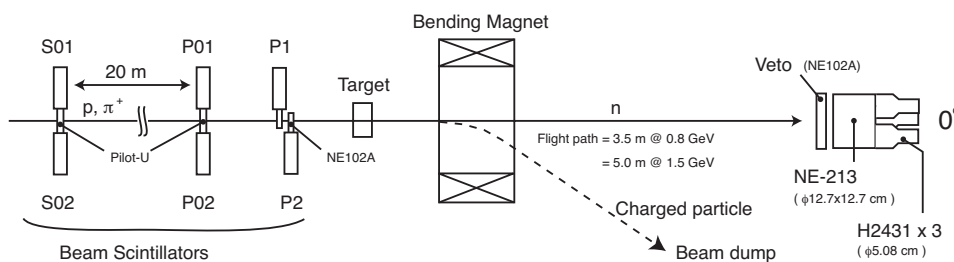


Fig. 1 Illustration of experimental arrangement.

### 3. Data analysis

Neutron spectra were obtained by subtracting the results of the target-out measurement from those of the target-in, after normalization with the number of incident protons. An example of the TOF spectra of the target-in and -out measurements by 0.8 GeV protons on Fe target is shown in Fig. 2, where the spectrum includes events of both neutrons and gamma-rays. The horizontal axis of the TOF spectrum was reversed, because the start signal for the TOF measurement was made at neutron detector. A sharp peak due to prompt gamma-rays was utilized as the time standard for converting TOF to emitted neutron energy. Prompt gamma peak is also presented in the results of target-out. The latter prompt gamma-rays came from the beam scintillators located at the upstream of the target, and were generated slightly prior to those from the target.

In usual TOF experiments using high-intensity pulsed beam, the time resolution is determined by the pulse width of the beam. However, the beam intensity at  $\pi 2$  beam line was very weak in a level of about  $10^5$  particles/2.5 s, and incident protons were individually counted in this measurement. Hence, the uncertainty of TOF came from the resolution of the detectors. The energy resolution for this experiment is shown in Fig. 3. In this figure, solid and dashed curves stand for the energy resolution of the NE213 scintillator with three H2431s and that with a Hamamatsu R1250 (rise time 2.5 ns) whose diameter is 12.7 cm, respectively. The energy resolution was obtained from the FWHM of the prompt gamma peak. The energy resolution of the NE213 scintillator with three H2431s is 100 MeV at 0.8 GeV and 55 % better than that with R1250. This resolution is better than other experiments[10] performed by NE213 scintillator with R1250, but about twice the value for the recoil proton spectrometer[15].

For high energy neutron incidence into NE213 scintillator, neutron events tend to overlap gamma ones, and then the pulse-shape discrimination (PSD) characteristics are deteriorated[16]. For this reason, the PSD technique was unusable for neutrons of interest in this measurement. Fortunately, most of gamma-rays have energies below several MeV. Then, we employed the higher-level bias setting, which is twice of the gamma-ray energy from Am-Be source (4.33 MeVee) to reduce the affect of the gamma-rays. Neutron detection efficiencies were calculated by the Monte Carlo code SCINFUL-QMD[17,18].

### 4. Results and discussion

Neutron-production double-differential cross-sections by 0.8 and 1.5 GeV protons on Fe and Pb targets are presented in Figs. 4 to 7. The bias level was set at twice the Am-Be threshold, 8.66 MeVee, because the main purpose of the experiment was the measurement of the neutrons above 100 MeV. Error-bars includes both

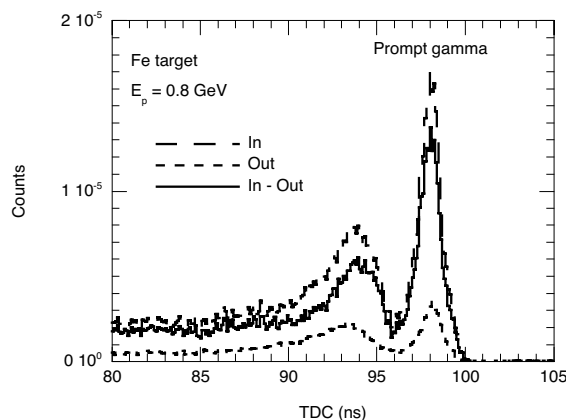


**Fig. 2** Time-of-flight (TOF) spectrum for neutrons and gamma-rays obtained by 0.8 GeV protons on iron target. Dashed and dotted lines indicate the results with target and without target, respectively. Solid line shows the difference between target-in and target-out events.

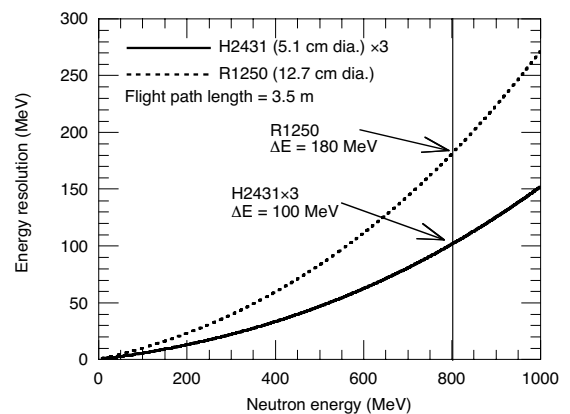


**Fig. 3** Energy resolution by two type of photomultipliers. Signals of three photomultipliers of H2431 were time-averaged for evaluating neutron arrival time.

statistical uncertainties and contiguity of neutron detection efficiency of 15 %. Experimental data are compared with other experimental data[11,12] measured by recoil proton spectrometers and the results of model calculation codes. The results of other experiments and calculation codes were broadened by Gaussian to fit to our energy resolution. The solid and dashed lines in Figs. 4(a) to 7(a) indicate the original values and the modified results, respectively. Our data were compared with the modified results in Figs. 4(b) to 7(b). Solid lines show the calculation results of the NMTC/JAM[13]. NMTC of this version adopts the inmedium nucleon-nucleon elastic scattering cross-sections of Cugnon[19,20]. Dashed lines indicate the calculation results of JQMD[14], which incorporates QMD with Statistical Decay Model (SDM) model. The experimental data obtained by Leray et al.[12] are exhibited in Figs. 4(b) and 5(b) with chain lines. The data by Bonner et al.[11] are also shown in Fig. 5(b) with dotted line. The cross-sections consist of two main components. The peak close to the energy of incident protons corresponds to quasi-elastic (charge exchange; CEX) nucleon-nucleon collisions. The lower broad peak positioning around 3/4 of incident energy is ascribed to pion-associated neutrons via the  $\Delta$ -resonance excitation in inelastic nucleon-nucleon collisions.

In Figs. 4(b) and 5(b) for the 0.8 GeV proton incidence, the experimental data exhibit both the CEX and pion-associated peak. For the Fe target, our data show good agreement with the experimental results of Leray et al. in the pion-associated region, although slightly smaller in the CEX region. For the Pb target, in the CEX region, the experimental data agree with the predictions of NMTC/JAM well. On the contrary, the absolute values of other experiments are 45 % larger than the results of our experiment. Below 250 MeV, the experimental data tend to include the neutrons scattered from the bending magnet pole piece. The effect is clear for Fe which has relatively low cross section in this energy region. In Figs. 6(b) and 7(b) for the 1.5 GeV proton incidence, the experimental data exhibit the pion-associated peak. However, the CEX peak does not appear due to the deterioration of the energy resolution. The absolute values at the pion-associated region are larger than JQMD and smaller than NMTC/JAM. Below 500 MeV, the experimental data tend to give larger values than code predictions. There is a possibility that the experimental data indicated with open circles contain the affection caused by the scattering at the bending magnet. For both 0.8 and 1.5 GeV proton incidence, the calculation results of NMTC/JAM show the remarkable overestimation at the pion-associated peak. This overestimation may be explained by an excessive forward angular distribution of  $\Delta$  particles adopted in the INC code. In contrast, the results of JQMD are in better agreement with experimental data at the pion-associated peak. However, JQMD does not exhibit the CEX peak.

## 5. Conclusion

The neutron-production double-differential cross sections were measured for 0.8 and 1.5 GeV protons incident on Fe and Pb targets. The high-resolution TOF method was adopted to determine the neutron energy. Three rapid-rise-time photomultipliers were connected with an NE213 scintillator to improve energy resolution in the measurement. For 0.8 GeV proton incidence, the CEX peak was identified by the high-resolution TOF method. Our experimental data agree with the results of NMTC/JAM in the CEX region. The discrepancy between the experimental data and those obtained by Leray et al. are less than 30 % in the pion-associated regions. For 1.5 GeV proton incidence, the results give middle values between NMTC/JAM and JQMD predictions in the pion-associated region. Present data exhibit the predictive capability of these models is not yet sufficient. NMTC/JAM show the abnormal pion-associated peak due to the inappropriate angular distribution of  $\Delta$  particle.

## Acknowledgement

The authors express their gratitude to Prof. Y. Yoshimura, Mr. M. Taino and the beam channel staff of KEK for their continuous encouragement and generous support of the experiment.

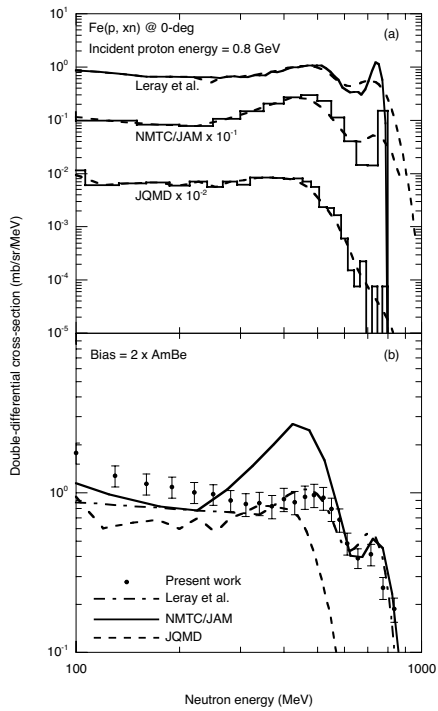


**Fig. 4** Neutron-production double-differential cross-sections for 0.8 GeV protons on iron target. The upper figure of (a) shows original values and modified results adjusted to fit the present experimental energy resolution. Comparison between our experimental data and modified results is shown in the lower figure of (b). Marks exhibit our experimental data. Solid and dashed lines present the results by NMTC/JAM and JQMD, respectively. Chain line indicates the experimental data by Leray et al.

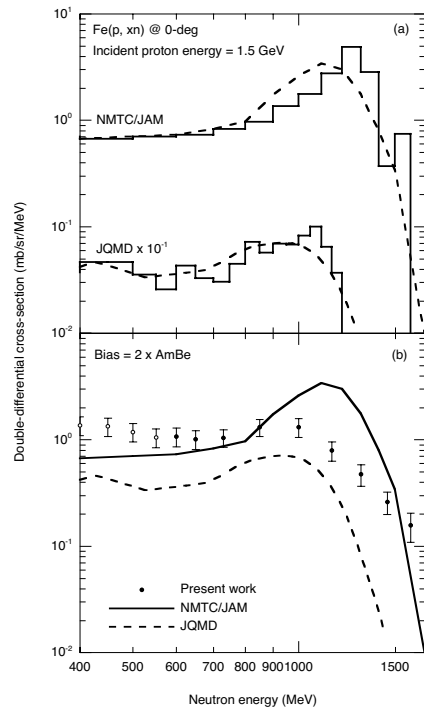


**Fig. 6** Neutron-production double-differential cross-sections for 1.5 GeV protons on Fe target. Marks indicates experimental data. Solid and dashed lines present the results by NMTC/JAM and JQMD, respectively.

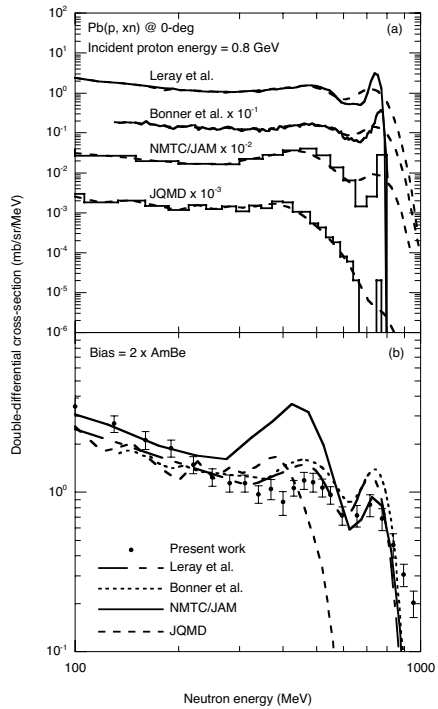


**Fig. 5** Same as for Fig. 4, except for lead target. Dotted line indicates the experimental data by Bonner et al.

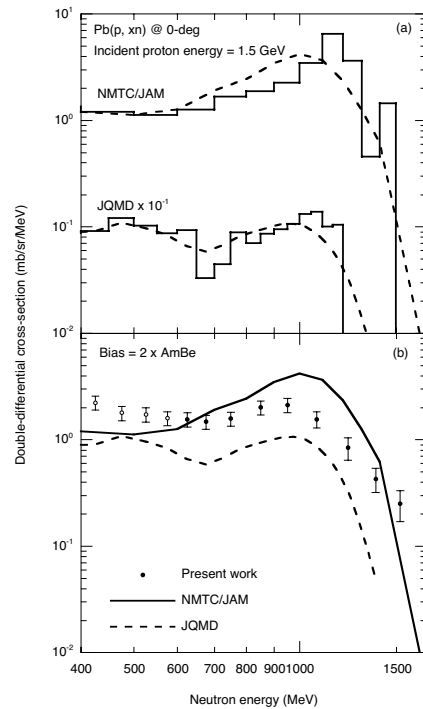


**Fig. 7** Same as for Fig. 6, except for Pb target.

## References

- [1] The Joint Project Team of JAERI and KEK, *The Joint Project for High-Intensity Proton Accelerators*, JAERI-Tech 99-056, Japan Atomic Energy Research Institute (JAERI), (1999).
- [2] *Conceptual Design Report, National Spallation Neutron Source*, NSNS/CDR-2/V1 and NSNS/CDR-2/V2, vols. **1** and **2**, Oak Ridge National Laboratory (ORNL), (1997).
- [3] G. Bauer, *The ESS Target Station Concept*, ESS-96-60T (1996).
- [4] T. Fukahori, Y. Watanabe, N. Yoshizawa, et al., "JENDL High Energy File," *J. Nucl. Sci. Technol.*, Supplement **2**, 25 (2002).
- [5] M. B. Chadwick, P. G. Young, R. E. MacFarlane, et al., *LA150 Documentation of Cross Sections, Heating, and Damage*, Los Alamos National Laboratory Report LA-UR-99-1222, Los Alamos National Laboratory (LANL), (1999).
- [6] Yu. N. Shubin, V. P. Lunev, A. Yu. Konobeyev, et al., *Cross section data library MENDL-2 to study activation as transmutation of materials irradiated by nucleons of intermediate energies*, report INDC(CCP)-385, International Atomic Energy Agency, (1995).
- [7] H. W. Bertini, "Intranuclear-cascade calculation of the secondary nucleon spectra from nucleon-nucleus interactions in the energy range 340 to 2900 MeV and comparisons with experiment," *Phys. Rev.*, **188**, 1711 (1969).
- [8] J. Aichelin, "Quantum molecular dynamics - A dynamical microscopic  $n$ -body approach to investigate fragment formation and the nuclear equation of state in heavy ion collisions," *Phys. Rep.*, **202**, 233 (1991).
- [9] T. Nakamoto, K. Ishibashi, N. Matsufuji, et al., "Spallation neutron measurement by the time-of-flight method with a short flight path," *J. Nucl. Sci. Technol.*, **32**, 827 (1995).
- [10] K. Ishibashi, H. Takada, T. Nakamoto, et al., "Measurement of neutron-production double-differential cross sections for nuclear spallation reaction induced by 0.8, 1.5 and 3.0 GeV protons," *J. Nucl. Sci. Technol.*, **34**, 529 (1997).
- [11] B. E. Bonner, J. E. Simmons, C. R. Newsom, et al., "Systematics of  $0^\circ$  neutron production by 800 MeV protons on targets with  $27 < A < 238$ ," *Phys. Rev.*, **18** (1978).
- [12] S. Leray, F. Borne, S. Crespin, et al., "Spallation neutron production by 0.8, 1.2, and 1.6 GeV protons on various targets," *Phys. Rev.*, **C65** (2002).
- [13] K. Niita, S. Meigo, H. Takada, et al., *High Energy Particle Transport Code NMTC/JAM*, JAERI-Data/Code 2001-007, Japan Atomic Energy Research Institute (JAERI), (2001).
- [14] K. Niita, T. Maruyama, Y. Nara, et al., *Development of JQMD (Jaeri Quantum Molecular Dynamics) Code*, JAERI-Data/Code 99-042, Japan Atomic Energy Research Institute (JAERI), (1999).
- [15] E. Martinez, J. Thun, Y. Patin, et al., "Spallation neutron spectra measurements Part II: Proton recoil spectrometer," *Nucl. Instrum. Method*, **A385**, 345 (1997).
- [16] Y. Iwamoto, D. Satoh, H. Kitsuki, et al., "Deterioration of pulse-shape discrimination in liquid organic scintillator at high energies," *2000 IEEE Nuclear Science Symposium Conference Record*, 6-215, (2001).
- [17] D. Satoh, N. Shigyo, Y. Iwamoto, et al., "Study of neutron detection efficiencies for liquid organic scintillator up to 3 GeV," *IEEE Trans. Nucl. Sci.*, **48**, 1165 (2001).
- [18] D. Satoh, S. Kunieda, Y. Iwamoto, et al., "Development of SCINFUL-QMD code to calculate the neutron detection efficiencies for liquid organic scintillator up to 3 GeV," *J. Nucl. Sci. Technol.*, Supplement **2**, 657 (2002).
- [19] J. Cugnon, "Monte carlo calculation of high-energy heavy-ion interactions," *Phys. Rev.*, **C22**, 1885 (1980).
- [20] J. Cugnon, T. Mizutani, J. Vandermeulen, "Equilibration in relativistic nuclear collisions. A monte carlo calculation," *Nucl. Phys.*, **A352**, 505 (1981).